Identification and Structural Ramifications of a Hinge Domain in Apolipoprotein A-I Discoidal High-density Lipoproteins of Different Size†

J. Nicholas Maiorano, Ronald J. Jandacek, Erica M. Horace, and W. Sean Davidson*

Department of Pathology and Laboratory Medicine, University of Cincinnati, 2120 East Galbraith Road, Cincinnati, Ohio 45237-0507

Received February 13, 2004; Revised Manuscript Received July 13, 2004

ABSTRACT: Apolipoprotein (apo) A-I is the major protein constituent of human high-density lipoprotein (HDL) and is likely responsible for many of its anti-atherogenic properties. Since distinct HDL size subspecies may play different roles in interactions critical for these properties, a key question concerns how apoA-I can adjust its conformation in response to changes in HDL particle size. A prominent hypothesis states that apoA-I contains a flexible "hinge domain" that can associate/dissociate from the lipoprotein as its diameter fluctuates. Although flexible domains clearly exist within HDL-bound apoA-I, this hypothesis has not been directly tested by assessing the ability of such domains to modulate their contacts with the lipid surface. In this work, discoidal HDL particles of different size were reconstituted with a series of human apoA-I mutants containing a single reporter tryptophan residue within each of its 22 amino acid amphipathic helical repeats. The particles also contained nitroxide spin labels, potent quenchers of tryptophan fluorescence, attached to the phospholipid acyl chains. We then measured the relative exposure of each tryptophan probe with increasing quencher concentrations. We found that, although there were modest structural changes across much of apoA-I, only helices 5, 6, and 7 exhibited significant differences in terms of exposure to lipid between large (96 Å) and small (78 Å) HDL particles. From these results, we present a model for a putative hinge domain in the context of recent "belt" and "hairpin" models of apoA-I structure in discoidal HDL particles.

Apolipoprotein (apo) A-I[1] is the major protein constituent of human high-density lipoprotein. Originally called apoGLN-1 because of its C-terminal glutamine residue (*1*), apoA-I has been intensively studied with the goal of understanding how its structure modulates HDL function. The 28 kDa single polypeptide is dominated by eight distinct 22 amino acid amphipathic helical domains which act as an interface between the hydrophobic regions of lipids and aqueous solvent (*2*). However, despite many years of study (for a review see ref 3), a partial crystal structure (*4*), and numerous detailed theoretical structure predictions (*5*−*7*), there is still relatively little that can be concretely stated about the structure of this protein in the spherical particles that make up the bulk of human HDL.

A key question that has yet to be unequivocally answered is how apoA-I can adjust its conformation to absorb or promote changes in HDL particle size, which can vary from 75 to 135 Å in diameter (*8*). There is strong evidence that certain size subspecies may play different roles in the interactions with membrane proteins and plasma factors in the circulation. For example, it is clear that lipid-poor species of apoA-I are the most efficient acceptors of cellular cholesterol via apolipoprotein-mediated cholesterol efflux (*9*, *10*). Furthermore, certain size classes of HDL are significantly better substrates for lecithin:cholesterol acyl transferase (LCAT) than others (*11*). Interestingly, the HDL size distribution is not continuous but clearly quantized into a number of discrete populations. Chung and colleagues (*8*) isolated and characterized these particles from human plasma and proposed that this size gradation was due to (a) the number of apolipoproteins associated with the particle and (b) the number of helical domains of apoA-I in contact with the lipid shell of the particle. It was proposed that amphipathic helical regions in the apoA-I sequence form a "hinge" domain that could provide a surface area buffering function in response to lipid composition changes in HDL (*12*). This idea was supported in studies of well-defined reconstituted HDL (rHDL) particles reconstituted from synthetic phospholipids, cholesterol, and purified apoA-I. Discoidal particles of 78 and 96 Å in diameter that each contained two apoA-I molecules could be accounted for by the removal of two putative helical domains from the edge of the smaller particles (*13*). Clues to the exact domains within apoA-I constituting the hinge came from limited proteolysis studies conducted by Kunitake et al. (*14*) and Dalton et al. (*15*).

† This work was supported in part by a RO1 (HL62542) grant from the National Heart Lung and Blood Institute (WSD).

* To whom correspondence should be addressed: Telephone: (513) 558-3707. Fax: (513) 558-1312. E-mail: Sean.Davidson@UC.edu.

[1] Abbreviations: Apo A-I, apolipoprotein A-I; FC, free (unesterified) cholesterol; GdnHCl, guanidine hydrochloride; HDL, high density lipoprotein; rHDL, reconstituted HDL; PAGGE, polyacrylamide gradient gel electrophoresis; PL, phospholipid; POPC, 1-palmitoyl, 2-oleoyl phosphatidylcholine; STB, standard Tris buffer; W@#, a single Trp mutant containing Trp at the amino acid with that position # with all other sites normally containing Trp converted to Phe; λ-max, wavelength of maximum fluorescence; WT, wild type.

10.1021/bi0496642 CCC: $27.50
Published on Web 08/26/2004

Both studies indicated that the region near amino acids 90−100 of apoA-I is more susceptible to proteolysis in small vs larger particles. In addition, monoclonal antibody studies indicated that the region between residues 99 and 143 exhibited increased epitope exposure in small vs large discoidal rHDL particles (*16*). Monoclonal antibody studies using reconstituted spherical particles also indicated that the regions 121−165 changed conformation in different sized reconstituted spherical particles (*17*). Unfortunately, these techniques are limited to detecting changes in protein conformation and cannot address whether the putative hinge domain can actually move off the edge of the particle.

In the current study, we used a fluorescence quenching approach to determine if a reporter tryptophan in the various helical domains of apoA-I actually becomes less associated with lipid in the smaller particles. We found that, although there were modest changes in conformation across most of apoA-I, the region between residues 130 and 174 (helices 5, 6 and 7) exhibited differences in exposure to lipid between large and small particles. We use this information to present a model for the putative hinge domain in the context of recent "belt" and "hairpin" models of apoA-I structure within discoidal rHDL particles.

EXPERIMENTAL PROCEDURES

Materials. Sodium deoxycholate, acrylamide, bovine serum albumin (BSA), azurin, and adrenocorticotropin hormone fragment 1−10 (SYSMEHFRWG) were purchased from Sigma Chemical Co. (St. Louis, MO) (+99% grade). 1-Palmitoyl, 2-oleoyl phosphatidylcholine (POPC), and the nitroxide spin probe 1-palmitoyl, 2-stearoyl(12-DOXYL)-sn-glycero-3-phosphocholine were purchased from Avanti Polar Lipids (Birmingham, AL). The atomic phosphorus standard was obtained from Sigma (St, Louis, MO). IgA protease (Igase) was obtained from Mobitec (Goettingen, Germany). All other reagents were of highest quality available.

Methods. Mutagenesis, Protein Expression, and Purification. The human proapoA-I cDNA in the pET30 (Novagen, Madison, WI) vector was used to generate single Trp mutants. Each of the five naturally occurring Trp residues (pos. −3 [in the pro segment], 8, 50, 72, 108) in proapoA-I were converted to Phe using site directed mutagenesis (Stratagene, La Jolla, CA), yielding a mutant that contained no Trp residues (W@ϕ). The W@X nomenclature states that a Trp residue has been introduced at position X and all other sites that normally contain a Trp residue in apoA-I have been converted to a Phe. We have demonstrated that these substitutions do not have major effects on the structure or function of the protein (*18*). To produce mutants of mature apoA-I that lacked the pro-segment, we added an Igase cleavage site to our expression vector between the pro-segment and the beginning of the mature gene (*19*). A Histidine tag (His-tag) was included on the N-terminus of the construct. Cleavage of the expression product at the Igase site removed the pro-segment and His-tag leaving a Thr-Pro on the N-terminus of the mature apoA-I protein. PCR based site-directed mutagenesis (QuickChange mutagenesis Kit, Stratagene, La Jolla, CA) was performed directly in the pET30 expression vector. W@ϕ was used as a template to insert a Trp residue at a position in the center of each of the 22 amino acid amphipathic α-helices in apoA-I (Figure 1). An additional mutant was also created with a single Trp near the C-terminal end of helix 5 (W@137). The sequences were verified on an Applied Biotechnology System DNA sequencer, University of Cincinnati DNA core.

Helix (mutant)		
	1	DEPPQSP
G*	8	WDRVKDLATVYDVLKDSGRDYVSQF
	34	EGSALGKQLN
1 (W@53)	44	LKLLDNWDSVTSTFSKLREQLG
2 (W@75)	66	PVTQEFWDNLEKETEGLRQEMS
3	88	KDLEEVKAKVQ
4 (W@108)	99	PYLDDFQKKWQEEMELYRQKVE
5 (W@130, 137)	121	PLRAELQEGARQKLHELQEKLS
6 (W@152)	143	PLGEEMRDRARAHVDALRTHLA
7 (W@174)	165	PYSDELRQRLAARLEALKENGG
8 (W@196)	187	ARLAEYHAKATEHLSTLSEKAK
9	209	PALEDLRQGLL
10 (W@229)	220	PVLESFKVSFLSALEEYTKKLN
	242	TQ

FIGURE 1: Amino acid sequence of human apoA-I and the location of Trp residue substitutions. The 10 predicted amphipathic α-helical domains are numbered on the left. The G* designation refers to the fact that this particular type of helix is commonly found in globular proteins (*43*). Helices 3 and 9 are putative 11-mer amphipathic helical repeats and the remaining 8 helices are the 22-mer amphipathic repeats that are likely responsible for the lipid binding functionality of apoA-I. The shaded residues illustrate the positions of a single Trp substitution on the hydrophobic face within each 22 amino acid repeat for the current studies. The figure and the helical numbering system is modified from Roberts et al. (*44*).

The resulting constructs were transfected into BL-21 (DE3) *E. coli* cells (Novagen, Madison, WI). The overexpression of the mutant apoA-I was performed using freshly transfected cells as described previously (*18*). After harvesting, the cells were resuspended in His binding buffer (20 mM Tris, 0.5 M NaCl, 5 mM imidazole, and 3 M guanidine HCL). The cells were lysed by sonication and the soluble cell contents were applied to a His-bind column (Novagen, Madison, WI) and eluted according to manufacturer's instructions. The His-tagged proteins were dialyzed into 10 mM ammonium bicarbonate buffer (pH 8.0) and lyophilized. Lyophilized proteins were solubilized in 3 M guanidine HCl, dialyzed into standard Tris buffer (10 mM Tris buffer pH 8.0 containing 0.15 M NaCl, 1mM EDTA and 0.2% NaN_3) and the His-tag was then removed by cleavage with 1:2000 (w:w) IgA protease at 37 °C for 16 h. The His-tag was removed by hydrophobic interaction chromatography on a phenyl sepharose HiTrap (Amersham Pharmacia, Piscataway, NJ) column resulting in the final mature apoA-I protein. Proteins prepared by this method were >95% pure as visualized by SDS electrophoresis stained with coomassie blue and the yields were about 3−5 mg protein per 100 mL of culture.

Preparation and Characterization of the Lipid-Containing Particles. Reconstituted HDL (rHDL) particles were prepared as described previously (*20*) using palmitoyloleoyl phosphatidylcholine (POPC), mutant apoA-I, and spin-labeled phospholipids. All phospholipid stock solutions were assayed before the reconstitution by the phosphorus method of Sokolof and Rothblat (*21*). For the 98 Å particles that lacked the spin label quencher, initial lipid to protein molar ratios were 78:4:0:1 (POPC:unesterified cholesterol:12-nitroxide-

DSPC:apoA-I). Additional particles were reconstituted with the following compositions in order to generate particles containing 2, 5, and 10 mol % spin-labeled phospholipid (as a percent of total phospholipid): 76.4:4:1.6:1, 74.1:4:1.6:1, and 70.2:4:7.8:1. For the 78 Å particles, the beginning ratios were 30:2:0:1 and the labeled particles were 29.4:2:0.6:1, 28.5:2:1.5:1, and 27::2:3:1, respectively. Any unreacted protein and vesicular structures were removed by gel filtration chromatography on a Superdex 200 gel filtration column (Amersham Pharmacia, Piscataway, NJ) (*22*). The phosphorus assay and the Markwell modification of the Lowry protein assay (*23*) determined the final lipid and protein concentrations. Particle hydrodynamic diameters were measured by gradient native polyacrylamide electrophoresis (PhastSystem, Amersham Pharmacia, Piscataway, NJ) (*22*). The secondary structure content of the apoA-I in the rHDL particles was estimated by circular dichroism at 222 nm (Jasco J-720 spectropolarimeter) (*24*).

Fluorescence Spectroscopy. All fluorescence measurements were performed on a Photon Technology International Quantamaster spectrometer in photon counting mode. The emission and excitation band-passes were 3.0 nm. The excitation wavelength for all Trp studies was 295 nm in order to minimize the contribution of tyrosine fluorescence in apoA-I. The samples at 0.1 mg/mL in STB for all studies were measured at 25 °C in a semi-micro quartz cuvette. The emission spectra from 305 to 360 nm were corrected for the background fluorescence of buffer alone. Fluorescence quenching experiments were carried out using increasing concentrations of acrylamide (0−0.2 M). After correction for buffer effects, the quenching parameters were calculated using a Stern−Volmer analysis (*25*, *26*).

Analytical Methods. To determine if the rHDL reconstitution process affected the amount of nitroxide-labeled PL present in the particles, samples of the lipid mixture before the reconstitution and from final rHDL preparations (delipidated with chloroform/methanol) were quantified by gas chromatography. The samples were saponified to hydrolyze fatty acids and esterified with a methanolic solution of boron trifluoride. The methyl esters were extracted into 10 mL of hexane, and 1 μL of this solution was injected into a Shimadzu GC17A gas chromatograph equipped with a 0.32 mm i.d., 30 m length DB-23 column. This resulted in baseline separation of all normally occurring fatty acids, which were identified by comparison of retention times with those of authentic samples of fatty acid methyl esters. The retention times of methyloleate was 13.23 min and that of 12-nitroxide-methyl stearate was 21.43 min. The concentration of the fatty acids were quantified by integrating the areas of the response of the flame ionization detector.

RESULTS

Experimental Design. The goal of this study was to identify the regions that adjust the circumference of the apoA-I annulus at the disk edge when present on 96 or 78 Å discoidal rHDL particles. In 96 Å particles, we have previously shown that the fluorescence of Trp residues placed in the center of the hydrophobic face of all 22 amino acid helical domains in apoA-I was best quenched by resident nitroxide-labeled phospholipids that contain the spin label on the 12 carbon of the acyl chains (*27*). Therefore, we hypothesized that if certain helices move away from the disk edge in 78 Å particles then the Trp residues contained in these domains should be less sensitive to changes in nitroxide concentration within the particle than in the 96Å particles. To test this, we used eight mutants of apoA-I that contained a reporter Trp residue placed in each helical domain (Figure 1). These were reconstituted into homogeneous rHDL particles of both 96 and 78 Å diameters that contained increasing concentrations of 12-nitroxide labeled phospholipids.

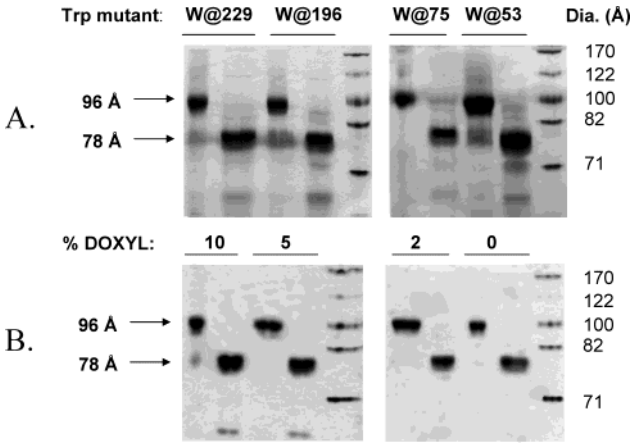

FIGURE 2: Native PAGE analysis of 96 and 78 Å rHDL particles generated with representative single Trp mutants (A) and with varying amounts of nitroxide-labeled phospholipid (B). Each gel is an 8−25% native polyacrylamide Phastgel (Amersham) stained with Coomassie blue. The molecular weight markers on the right side of all gels are Amersham HMW (Cat # 17-0445-01) shown with the corresponding hydrodynamic diameter (*45*). The rHDL particles were prepared as described in EXPERIMENTAL PROCEDURES. In panel A, particles of both sizes (after isolation by gel filtration) are shown for the single Trp mutants of apoA-I indicated above the lanes. These did not contain nitroxide-labeled phospholipids. In panel B, all particles shown were made with the same Trp mutant (W@108), but contain the mole fraction of DOXYL-labeled phospholipid (attached to carbon 12 of the sn-2 acyl chain) indicated above the lanes.

Characterization of the rHDL Particles. For each single Trp mutant shown in Figure 1, homogeneous rHDL particles were generated by the cholate dialysis method (*28*) under conditions that favor the formation of both 78 and 96Å rHDL particles (see EXPERIMENTAL PROCEDURES). These particles have been generated by many laboratories and have been well characterized to contain two molecules of apoA-I per particle (*13*, *22*, *29*). For each mutant particle of a given size, four separate preparations were generated that contained 0, 2, 5, or 10 mol % of 12-nitroxide labeled phospholipid. Using a gas chromatography based fatty acid analysis; we found that there was not a significant loss of the nitroxide label during the cholate removal procedure or the gel filtration purification of the particles (data not shown). Figure 2 shows a native PAGE analysis of a subset of the particles. Consistent with our previous results, we found that the amino acid substitutions required to make a single Trp mutant had no effect on the size or homogeneity of the particles (*27*) (Figure 2A). Furthermore, the presence of the 12-nitroxide-PL of up to 10 mol % also had no effect on these parameters (Figure 2B). A small amount of lipid-free apoA-I appeared in the lanes with the 78 Å particles. We believe that this occurred from apoA-I being stripped off the particles during electrophoresis because the free protein could not be detected

Table 1: Compositional Comparison of RHDL Particles Compared Across DOXYL Lipid Content and Across Trp Mutant Location

	PL:apoA-I ratio (mol/mol)[a]	
% DOXYL	77 Å rHDL	96 Å rHDL
0	30 ± 7[b]	77 ± 15
2	32 ± 5	74 ± 14
5	35 ± 7	76 ± 12
10	35 ± 9	74 ± 17
	$p = 0.30$ NS[c]	$p = 0.96$ NS
mutant	77 Å rHDL	96 Å rHDL
WT apoA-I	25 ± 2	75 ± 6
W@53	27 ± 9	60 ± 7*
W@75	21 ± 5	69 ± 12
W@108	27 ± 9	82 ± 13
W@130	21 ± 2	77 ± 8
W@137	26 ± 6	65 ± 9
W@152	31 ± 9	80 ± 2
W@174	25 ± 4	83 ±6
W@196	22 ± 2	71 ± 4
W@229	23 ± 1	69 ± 3
	$p > 0.05$ NS[d]	$p > 0.05$

[a] Total phospholipid to apoA-I molar ratio (including any nitroxide-labeled PL) measured as described in EXPERIMENTAL PROCEDURES. These particles also contained cholesterol. On average, the 96Å particles were found to contain 4−6 molecules of cholesterol per particle and the 78Å had 2−3 molecules per particle. There was no statistical difference in cholesterol content detected among the particles. [b] These average values were accumulated across all mutants within the indicated nitroxide-labeled PL concentration. The error is represented by a standard deviation derived from a total of n=27 determinations. In most cases, data is compared between experiments performed on different days. [c] To determine if the presence of the nitroxide label at various concentrations affected the composition of the particles, a one-way analysis of variance was performed on the values in the column directly above. $p < 0.05$ was considered to be indicative of a significant difference existing among all values. [d] To determine if the presence of a given mutation affected the composition of the particles, a one way analysis of variance was performed on the values in the column directly above. $p < 0.05$ was considered to be indicative of a significant difference existing among the data. The one case where a difference existed that was greater than predicted by chance is indicated with an asterisk.

by gel filtration analysis (data not shown). We have also demonstrated that neither the mutations nor the presence of the 12-nitroxide-PL affect the total α-helical content of these complexes (*20*, *27*). Table 1 compares the chemical compositions of the particles generated for this study. Within each size class, we were unable to detect a statistically significant difference between the phospholipid-to-protein ratios of the particles across all of the nitroxide PL concentrations used. Similarly, the particles within each size class made with the different single Trp mutants were found not to be significantly different from those created with the WT protein. A single exception was the W@53 mutant in the 96 Å particles. Although this difference was statistically significant in this particular study, we did not observe this effect in previous studies using the same mutant (*20*), and therefore, it is likely due to slight batch to batch variation in this particular mutant. These results indicate that, in general, the reporter residues and the quenching agents did not significantly change the properties of the particles and that our results can be applied to the WT situation.

Satisfied with the quality of the particles, we performed a battery of fluorescence experiments designed to probe the chemical environment of the Trp residue in each particle.

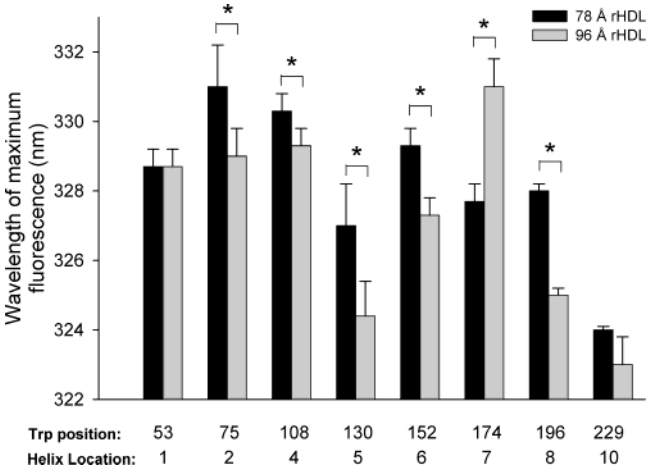

FIGURE 3: Wavelength of maximum fluorescence (λ-max) for single Trp mutants in 78 and 96 Å rHDL particles. For each particle, the λ-max was measured at 25 °C in STB. Each bar is the mean of 6 determinations and the error bar represents 1 sample standard deviation. Dark bars show the data for 78 Å particles and the gray bars show the 96 Å. The stars indicate a statistically significant differences existing between the two different sized particles generated with a given Trp mutant, as indicated by a paired t-test ($p < 0.05$).

Figure 3 shows the wavelength of maximum fluorescence (λ-max) measured for each complex. The λ-max is a measure of the polarity of the environment of the Trp residue. The Trp environment can range from hydrophobic, in which the residue is in contact with nonpolar regions of protein or with lipid, to hydrophilic, in which the Trp is near charged residues or exposed to the aqueous phase. Our previous work has shown that a typical λ-max for Trp residues in contact with lipid or hydrophobic sequestration within protein ranges from 324 to 336 nm (*18*, *27*). On the other hand, λ-max may be red shifted to values of about 354 nm for highly solvent exposed Trp residues such as found in the adrenocorticotropin hormone peptide (*18*). The majority of the rHDL particles of both sizes exhibited λ-max values consistent with lipid contact. Three exceptions were Trps 130, 196, and 229 in the 96 Å particles, which were more blue shifted, suggesting that they may be particularly tightly associated with lipid. Except Trps 53 and 229, all of the residues demonstrated statistically significant changes in environment when compared with the two particle sizes. However, these changes were extremely small when compared to the full range of possible changes in the hydrophobicity of the Trp environment as exemplified by the adrenocorticotropin hormone peptide. In most cases, the environment became slightly more polar in the 78 Å particles. However, Trp 174 in helix 7 slightly decreased its polarity in the smaller particles. These data suggest that conformational differences within apoA-I between the two particles can modestly affect the chemical environment of Trp residues across most of the molecule, but no gross changes in the hydrophobicity of the environment were apparent.

Because the λ-max can be affected by both solvent exposure and/or contacts with polar protein domains, we performed acrylamide quenching experiments to focus on the relative exposure of the Trp residues to solvent. Solvent exposed Trp residues collide with soluble acrylamide resulting in a nonradiative relaxation of the excited state. The Stern−Volmer constant (Ksv) quantitates the accessibility

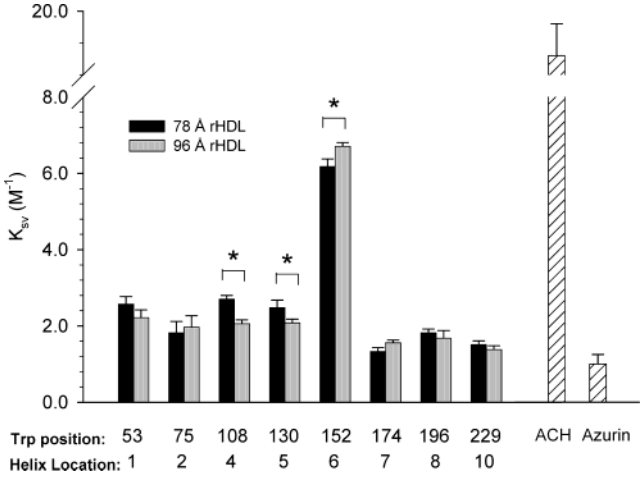

FIGURE 4: Acrylamide quenching of single Trp mutants in 78 and 96 Å rHDL particles. The *Y*-axis is the steady-state Stern−Volmer constant (Ksv) representing the accessibility of a particular Trp residue to acrylamide in the aqueous milieu. Each bar is the mean of 3 determinations and the error bar represents 1 sample standard deviation. Dark bars show the data for 78 Å particles and the gray bars show the 96 Å. The stars indicate a statistically significant differences existing between the two different sized particles generated with a given Trp mutant, as indicated by a paired t-test where $p<0.05$. The data in the hatched bars show the results from two control proteins; adrenochorticotropin hormone (ACH) contains a single Trp residue that is highly exposed to solvent whereas the Trp residue in azurin is almost completely solvent inaccessible (*30*).

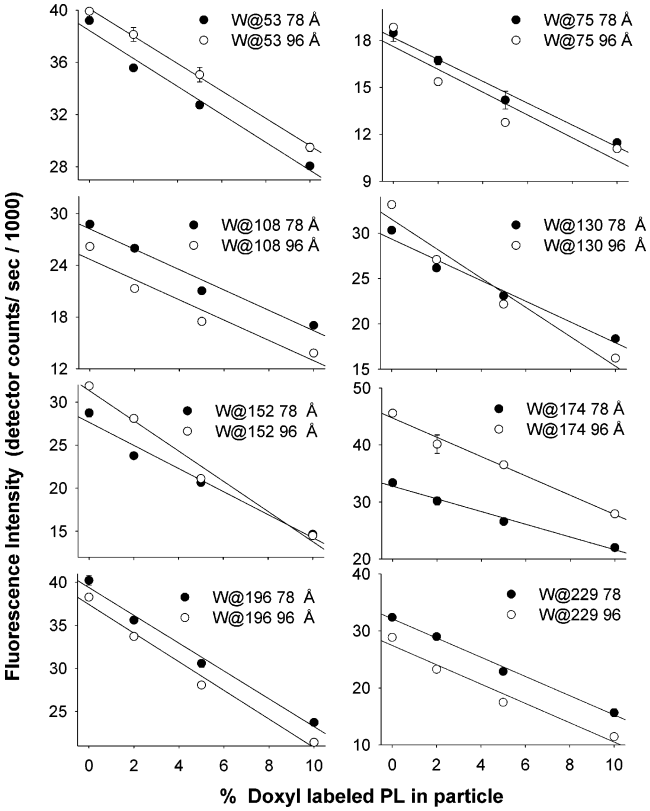

FIGURE 5: Effect of increasing fraction of 12-nitroxide-labeled phospholipid on the fluorescence intensity of single Trp mutants in 78 and 96 Å particles. The fluorescence intensity monitored at the l-max was measured for both size particles containing 0, 2, 5 or 10 mol % 12-nitroxide-labeled phospholipid under the same conditions as listed in Figure 3. For each mutant indicated, the filled circles represent the 78 Å particle and the open circles show the 96 Å. For each size particle, a least squares linear regression is drawn through the points. Each point is the mean from 3 determinations and the error bars represent 1 S. D.

of the Trp residues to the quencher. A low Ksv indicates nonsolvated environments; high values indicate high solvent exposure. Figure 4 shows that the control protein azurin (a protein with a highly solvent protected Trp residue (*30*)) exhibited a low Ksv as expected. The highly exposed Trp in ACH peptide was easily quenched and gave a Ksv of about 18/M. In general, the apoA-I mutant particles exhibited protected Trp environments with Ksv values closer to that of azurin than that of the ACH peptide. However, when compared between the two particle sizes, only residues 108, 130, and 152 demonstrated statistically different solvent exposures in the 78 Å particles with Trps 108 and 130 becoming modestly more exposed and Trp 152 becoming less exposed. These changes, although statistically significant, were also relatively minor when compared to the solvent exposed control.

We next determined the exposure of each Trp residue to the lipid contained in the rHDL particle. The panels in Figure 5 show the fluorescence intensity of each particle as a function of the molar % of nitroxide-PL present. For the mutant W@53, it is clear that the 96 Å particles without 12-nitroxide-PL exhibited a high fluorescence intensity. This decreased linearly as the quenching agent was titrated into the particles. The 78 Å particles made with W@53 exhibited an almost identical pattern of quenching. In contrast, the quenching profiles for the W@130 mutant were quite different for the two particle sizes with the 78 Å particle being less sensitive to the increasing presence of the quencher. The slopes of the linear regressions through all the plots are listed in Table 2 to quantitate the relative susceptibility of each probe to the quencher. A statistical comparison was performed to compare the slopes within a given mutant between the particle sizes. It is clear that the

Table 2: Effect of Nitroxide Labeled Phospholipid Concentration on the Fluorescence Intensity of Trp Residues in Each Helical Domain of ApoA-I

mutant	slope for 78 Å rHDL[a]	slope for 96 Å rHDL	*P* value[b]
W@53	−1097 ± 26	−1075 ± 65	0.66
W@75	−721 ± 12	−728 ± 4	0.90
W@108	−1181 ± 40	−1176 ± 6	0.85
W@130	−1171 ± 20	−1550 ± 11	0.001*
W@137	−1153 ± 53	−1364 ± 50	0.049*
W@152	−1339 ± 35	−1552 ± 23	0.002*
W@174	−1116 ± 6	−1693 ±111	0.01*
W@196	−1551 ± 54	−1584 ± 6	0.44
W@229	−1913 ± 68	−1866 ± 35	0.37

[a] The value is the slope of the line in Figure 5 that represents the susceptibility of a given Trp residue to quenching by the nitroxide-labeled PL in the particle. A more pronounced negative slope suggests higher exposure to the quenching agent. Units are counts/sec/% nitroxide labeled PL. The error is one standard deviation from 3 observations. [b] The value is a p-value obtained from a paired t-test. Within a given mutant, the slopes for the 78 Å rHDL were compared with that for the 96 Å rHDL. A *p* value of <0.05 indicated a statistically significant difference and is distinguished by an asterisk.

Trp residues contained in helices 5, 6, and 7 exhibited significant differences with a lower Trp susceptibility to lipid based quenching in the small particles whereas the others did not.

To further verify the results in Figure 5 and Table 2, we generated an additional Trp mutant. We placed a Trp at

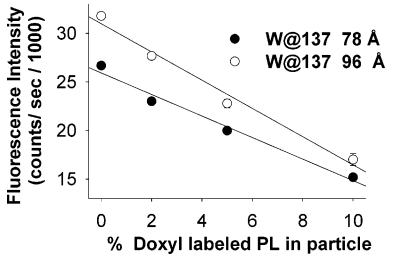

FIGURE 6: Lipid exposure of W@137 (at the end of helix 5) in 78 and 96 Å rHDL particles. This figure is organized similarly to Figure 5. For each mutant indicated, the filled circles represent the 78 Å particle and the open circles show the 96 Å. Each point is the mean from 3 determinations and the error bars represent 1 S. D.

position 137 in helix 5 (Figure 1). This residue was also located on the hydrophobic face but is two helical turns C-terminal to Trp 130. We performed the same lipid-based quenching experiments on this mutant and the results are shown in Figure 6. Again, Trp 137 in the 78 Å particle was less sensitive to the increasing concentrations of the nitroxide-PL than in the 96 Å particle. The statistical comparison of the slopes has been included in Table 2. These data indicate that the changes in Trp exposure shown in Table 2 are not due to some peculiarity with Trp residues located only in the center of the helix.

DISCUSSION

The data reported here show that Trp residues in putative helical domains 5, 6, and 7 of apoA-I exhibit reduced sensitivity to lipid-associated nitroxide quenching agents within 78 Å reconstituted HDL particles vs those in 96 Å particles. Interestingly, the changes in lipid exposure were not accompanied by profound changes in the hydrophobic environments of the Trp residues. Although many of the Trp residues studied exhibited statistically significant changes in WMF or Ksv, these changes were rather modest on the larger scale of potential Trp hydrophobicity ranges. For example, fully solvated Trp residues exhibit a WMF around 354 nm, whereas Trp residues involved in protective protein:protein or protein:lipid contacts range from 324 to 336 nm (*27*). It is clear from Figure 3 that none of the Trp residues studied underwent a major change in hydrophobic environment between the two sized particles, as all were within the range commonly found for protein or lipid sequestered Trp residues. Similarly, although some of the Trp residues exhibited statistically significant changes in acrylamide exposure, these were also small compared to the full range of potential solvent accessibility illustrated by the Ksv of the adrenocorticotropin hormone peptide. This suggests that a Trp residue that is buried in lipid in a 96 Å particle likely seeks out protective protein:protein interactions once it is forced off the disk edge in a smaller particle as part of a hinge domain. Thus, relatively minor changes in the WMF or Ksv values are expected, especially since the Trp residues were all placed on the hydrophobic faces of the putative amphipathic helices. By contrast, a Trp residue *must* exhibit a reduction in lipid exposure if it is part of a domain that moves away from the lipid. This study demonstrated significant and reproducible reductions in lipid exposure for Trp residues in only 3 of the eight 22 amino acid helices within apoA-I in the 78 Å particles. The exposures of the remaining 5 Trp residues were identical between the two sized particles. The three helices that exhibited the change were all adjacent to each other in the primary sequence and in the same region known to undergo significant changes in epitope expression between different sized particles (*16*). In addition, Sorci-Thomas et al. have demonstrated that the regions encompassing helices 6 and 7 are key interaction sites for lecithin:cholesterol acyltransferase (*31*, *32*). Therefore, our data is consistent with the fact that the 78 Å particles are much poorer activators of this enzyme than the 96 Å particles (*33*). Furthermore, we went back and put another Trp residue at a different location within this region and obtained similar results. This implies that helices 5, 6, and/or 7 may act like a spring to either dissociate from the disk edge in situations of decreasing particle circumference or associate upon increases.

Our data places this movable domain between residues 130 and 174. This is closer to C-terminus than suggested by some other studies. For example, Corsico et al. (*34*) utilized photoactivatable labeling reagents contained on the polar headgroups of phospholipid molecules to propose that the region between residues 87 and 112 of apoA-I can dissociate from the edge of an rHDL disk and then interact with vesicle membrane surfaces. This domain is similar to a region immediately C-terminal to residue 100 that is highly sensitive to proteolytic cleavage in discoidal particles (*14*, *15*). However, in our study, Trp 108 showed no change in sensitivity to the nitroxide phospholipids in either sized particle in our system. Furthermore, we have previously demonstrated that Trp 108 does not change position with respect to the bilayer between these two sized particles (*20*). Since the labeling groups used in the Corsico study were situated in the headgroup region of the phospholipid bilayer, we propose the possibility that the interaction of a more C-terminal region with the vesicular surface may allow the rather accessible domain near residue 100 to be easily modified by the labeling reagent without it being a hinge domain itself. This may explain why the authors did not see quenching of Trp fluorescence when a quencher was placed on the phospholipid acyl chains but did see quenching when bilayer surface quenching agents were used (*34*). This study, as well as studies using proteolytic sensitivity and epitope exposure, are based on the strategy of detecting *increased* exposure of a given protein domain to reagents that interact from the *outside* of the rHDL particle. Therefore, one could argue that these approaches could be sensitive to highly exposed sites on lipid-bound apoA-I that may not necessarily move away from the particle edge. By contrast, this study measured *decreased* exposure of a domain from reagents located *inside* the particle. Although our approach cannot address the final destination of the domain, we would argue that our results provide direct evidence that the 130−174 domain moves away from the disk edge in addition to undergoing a conformation change that can be measured by antibody binding (*16*), at least when transitioning between the two particle diameters we studied. A possible alternative interpretation of our data is that apoA-I can adjust its circumference by unfolding a series of small domains, rather than a single large domain composed of two helices. Although we cannot conclusively rule this out, we suggest that the fact that all four movable Trp residues were located on adjacent putative helical segments argues more strongly

Table 3: Geometric Parameters of 96 and 78 Å Discoidal RHDL Particles

particle diameter (Å)	lipid patch diameter (Å)[a]	circumference covered by protein (Å)[b]	helical amino acids required[c]	22 a. a. helical segments required (per mol apoA-I)
96	81	255	170	7.8
78	63	198	132	6.0

[a] Assuming 15 Å for the protein encapsulating the lipid patch. This is an average value based on 10 (5) and 20 Å (42). [b] Calculated using the radius of the lipid patch (r) and $2\pi r^2$. [c] Assuming 1.5 Å per residue in an α helix.

for the presence of a single domain encompassing all the Trp residues.

Structural Ramifications of a Movable Domain in Discoidal rHDL. It is widely accepted that discoidal HDL particles exist as a disk of phospholipid/cholesterol bilayer that is surrounded at its edges by the amphipathic helices of apoA-I. The particles in this study contained exactly two molecules of apoA-I per particle (*13*). Table 3 lists some basic geometric parameters of these complexes. Taking the case of the 96 Å particle first, a lipid patch circumference of 255 Å requires approximately 170 α-helical residues per face to cover the phospholipid acyl chains, assuming the standard 1.5 Å per residue in a standard α-helix. Therefore, about eight 22 amino acid helical segments are required per molecule of apoA-I to be in contact with lipid (*13*). This value is consistent with experimentally determined α-helical values for apoA-I in 96 Å particles measured by circular dichroism. Similar calculations for the 78 Å particles yield about six 22 amino acid helical segments that are in contact with the lipid per molecule of apoA-I. Therefore, between the large and the small disks, each of the two resident molecules of apoA-I must exclude about 2 helical domains from the disk edge.

Segrest et al. (*35*, *36*) first proposed that the α-helices of apoA-I were arranged around the circumference of discoidal HDL with the long axis of the helices perpendicular to the phospholipid acyl chains. This is generally known as the "belt" model. This group (*6*) recently published a computer prediction termed the "double belt" model for a reconstituted HDL particle. In this model, two ring-shaped molecules of apoA-I are stacked on top of each other with both forming nearly continuous helices that wrap around the disk in an antiparallel orientation on each leaflet of the membrane (Figure 7, top). Computer analysis identified a particular registry between the monomers resulting in the highest number of possible interhelical salt bridge connections between the two molecules, suggesting that the helices may spend much of their time in this registry. An alternative belt-like model, initially suggested by Brouillette et al. (*3*), predicts that all molecules on a given particle are arranged in a hairpin orientation (Figure 8, top). In this model, about half of the molecule is on one leaflet and, after a turn, the other half proceeds antiparallel to the first on the opposing leaflet. This model preserves the potential for salt bridge interactions between the same residues as the double belt, although these occur intramolecularly in the hairpin. There is ample recent evidence that indicates that the helices of apoA-I lie in a belt orientation of some type (*20*, *27*, *37*, *38*). We recently combined chemical cross linking with high-resolution mass spectrometry analyses to confirm the helix registry that is predicted by both the double belt and hairpin belt models (*39*) in the 96 Å disks. Unfortunately, the study was not able to conclusively distinguish between the two models. Therefore, we discuss the implications of the proposed movement of helices 5, 6, and/or 7 in the context of both models.

We begin with some simple assumptions. First, we assumed that a hinge domain should consist of about two helical domains (about 44 helical residues) per molecule of apoA-I. Second, we assumed that the decrease in helicity that occurs in apoA-I between the 96 and 78 Å particles (about −11% (*40*)) occurs in this region, i.e., this region exists as helices in the 96 Å particle and as random coil in the 78 Å particles. Third, it was assumed that this region dissociates from the disk edge in the 78 Å particles. Finally, in the absence of experimental helical registry data in the 78 Å particles, each model was drawn to preserve the maximum possible number of interhelical salt bridge interactions known to be present in the 96 Å particle (*6*, *39*).

Double Belt Model. Figure 7 (top) shows the case for the double belt model in a 96Å rHDL particle in which both molecules of apoA-I are represented as if taken from the edge of the disk and laid flat on the paper or screen in their predicted registry. Figure 7A shows a model for the 78 Å particle in which helices 5 and 6 were removed from the disk edge as random coil in both copies of apoA-I. These were chosen because of all three fluorescence measurements implicated this region as undergoing changes in Trp environment between the different size particles. Because residue 174 in helix 7 was implicated in two of the three measurements (including the more critical nitroxide exposure studies, see above), Figure 7B shows another model that includes Trp residues 130, 137, 152, and 174. To remove only 2 helices from the disk edge, all of helix 6 and the C- and N-terminal halves of helices 5 and 6 were moved. Although the models initially appear similar, the consequences for maintaining the salt bridge interactions that are observed in the 96 Å particle differ. In model A, we estimate that about 14 of the original 23 salt bridge opportunities remain viable in the 78 Å particles. In model B, only 8 of the original possibilities are maintained. In addition, both models predict the possibility for new helical associations between helix 4 on both molecules as well as between helices 5 and 3 in model B.

Helical Hairpin Model. As described above, the helical hairpin model also allows for similar helical salt bridge interactions as the double belt model (Figure 8, top). Figure 8A shows the case when helices 5 and 6 are removed. Figure 8B shows the case when the Trp from helix 7 is included in the hinge region. In each case, A or B, the hairpin models exhibit the same potential for conservation of the salt bridges that occurred in the corresponding double belt model with the difference being the intramolecular nature of the contacts.

The exclusion of helix 7 from the movable hinge might be conceptually more satisfying because it allows for the movement of two discrete helical domains that are punctuated with "kink inducing" proline residues instead of the arbitrary breaking of two potential helical domains somewhere in the middle. The Trp residue in helix 7 did undergo a change in its exposure to the nitroxide spin label on the phospholipid at position 12, but it did not become more exposed to solvent. A possible explanation for this result may be that the

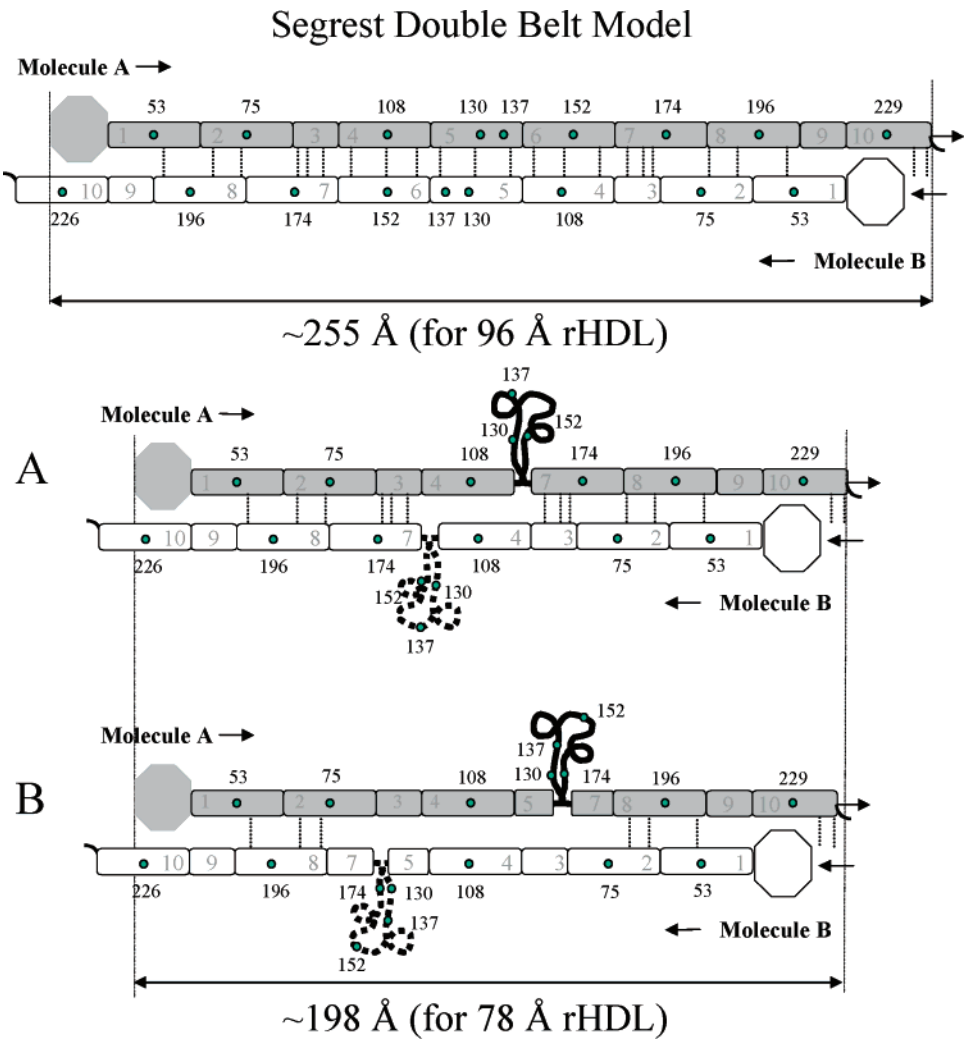

FIGURE 7: Potential double belt models for the 78 Å rHDL particles. Two molecules of apoA-I are represented as either gray (molecule A) or white (molecule B) as if they had been taken off of the edge of a three-dimensional rHDL disk and laid flat on the paper or screen. (Top) The double belt model for a 96 Å rHDL particle. The registry of the helices is shown in the 5/5 antiparallel orientation as modeled by Segrest et al. (*6*). Residues 1−44 are predicted to exist in a globular conformation and are represented as an octagon. Each amphipathic helical segment is represented as a rectangle and is numbered according to the scheme outlined in Figure 1. The individual Trp residues are shown as numbered dots in their approximate location along each molecule. (A) A model for the 78 Å particle in which helices 5 and 6 only have been removed from the disk edge and represented as random coil (solid black line). (B) A model that includes the Trp residue in helix 7 as part of the hinge domain. All of helix 6 and the C- and N-terminal halves of helices 5 and 6 included. All models for the 78 Å particles are drawn to preserve the maximum number of putative salt bridge interactions (*6*) that are predicted to be present in the 96 Å particles (dotted lines drawn between the molecules).

movement of the hinge helices 5 and 6 away from the disk edge caused a shift in the position of helix 7 in the bilayer rather than its complete removal. Perhaps it moves closer to the headgroup region of the phospholipids while still maintaining contact with the lipid acyl chains when the hinge is extended. To address this possibility, we performed experiments with the W@174 mutant using nitroxide spin labels that were situated at the 5 carbon position of the phospholipid acyl chain (data not shown). The results indicated that this residue as very weakly quenched at this position in either sized particle, arguing that it does indeed leave the edge of the particle without shifting to a shallower position on the bilayer. Therefore, we would argue that the models shown in case B in Figures 7 and 8 are the simplest models that account for our data. The possibility remains, however, that the interhelical salt bridge pairings that are known to be present in the 96 Å particles may be completely different in the 78 Å particles. This is plausible considering that there is evidence for helical registry shifts within the 96 Å particles themselves (*4*, *41*). Indeed, it is attractive to postulate that the hinge domains on each molecule of apoA-I may orient themselves in direct opposition in order to participate in protein−protein interactions that stabilize the dissociated regions. This would account for the rather modest changes in the WMF and acrylamide quenching values we measured. Such an association could occur in the hairpin models, but will likely require a significant shift in the helical registry for the double belt models.

It is clear that more information on the helical registry for apoA-I molecules in the 78Å particles is required. Whatever the exact registry of these domains, it is clear that the region from about amino acid 130 through 174 of apoA-I is dynamic and likely an important area of conformational flexibility that modulates HDL size. Although our experiments did not study spherical HDL particles, studies by Curtiss et al. (*17*) suggest that a similar region (121−165)

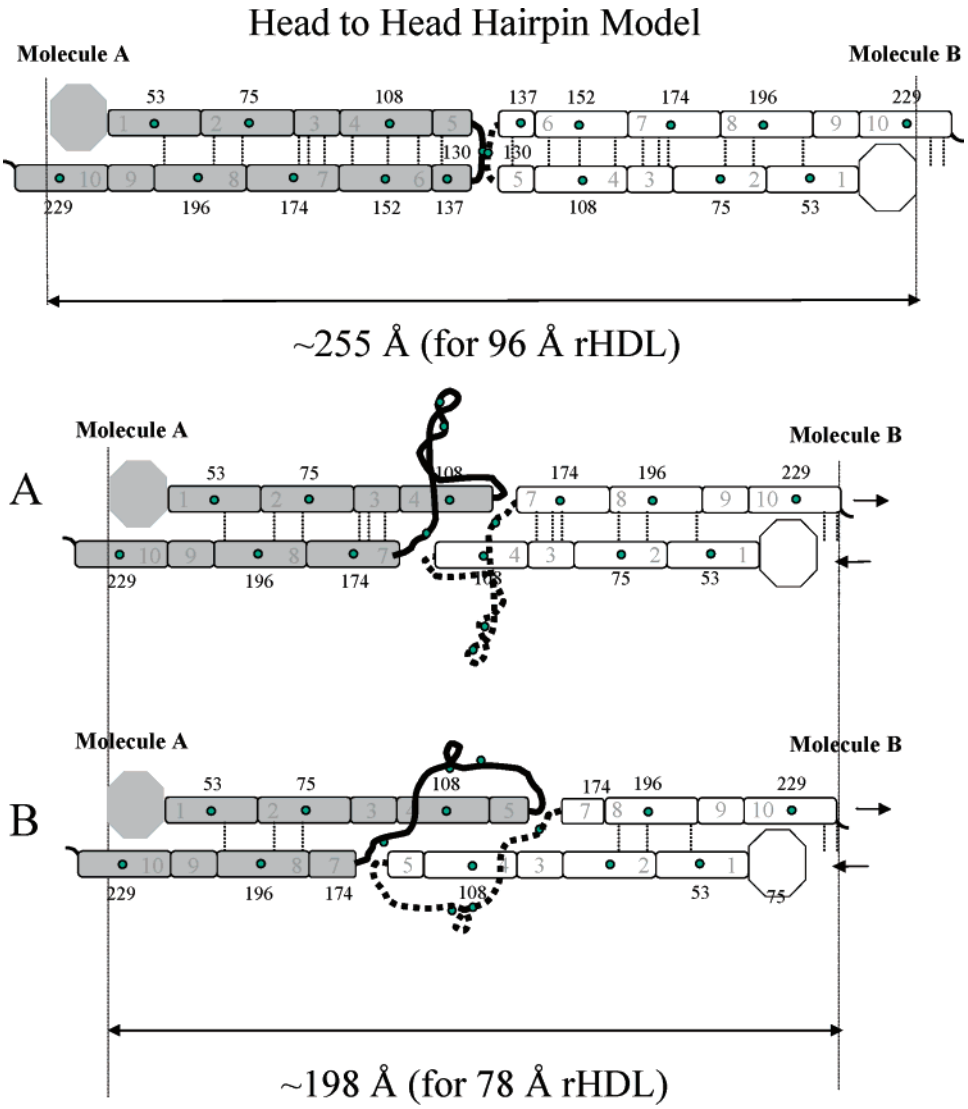

FIGURE 8: Potential hairpin belt models for the 78Å rHDL particles. This figure is organized similarly to Figure 7. (Top) A hairpin belt model proposed for the 96 Å rHDL particles in the same helix registry as for the double belt model. (A) A model for the 78 Å particle in which helices 5 and 6 only have been removed from the disk edge and represented as random coil (solid black line). (B) A model that includes the Trp residue in helix 7 as part of the hinge domain. All of helix 6 and the C- and N-terminal halves of helices 5 and 6 included. All models for the 78 Å particles are drawn to preserve the maximum number of putative salt bridge interactions (*6*) that are predicted to be present in the 96 Å particles (dotted lines drawn between the molecules).

may also be critical for this function in spherical HDL particles such as those of human plasma.

REFERENCES

1. Shore, B., and Shore, V. (1969) Isolation and characterization of polypeptides of human serum lipoproteins. *Biochemistry 8*, 4510−4516.
2. Segrest, J. P., Jackson, R. L., Morrisett, J. D., and Gotto, A. M. J. (1974) A molecular theory of lipid−protein interactions in the plasma lipoproteins. *FEBS Lett. 38*, 247−258.
3. Brouillette, C. G., and Anantharamaiah, G. M. (1995) Structural models of human apolipoprotein A-I. [Review]. *Biochim. Biophys. Acta 1256*, 103−129.
4. Borhani, D. W., Rogers, D. P., Engler, J. A., and Brouillette, C. G. (1997) Crystal structure of truncated human apolipoprotein A-I suggests a lipid-bound conformation. *Proc. Natl. Acad. Sci. U.S.A. 94*, 12291−12296.
5. Phillips, J. C., Wriggers, W., Li, Z., Jonas, A., and Schulten, K. (1997) Predicting the structure of apolipoprotein A-I in reconstituted high-density lipoprotein disks. *Biophys. J. 73*, 2337−2346.
6. Segrest, J. P., Jones, M. K., Klon, A. E., Sheldahl, C. J., Hellinger, M., De Loof, H., and Harvey, S. C. (1999) A detailed molecular belt model for apolipoprotein A-I in discoidal high-density lipoprotein. *J. Biol. Chem. 274*, 31755−31758.
7. Klon, A. E., Segrest, J. P., and Harvey, S. C. (2002) Comparative models for human apolipoprotein A-I bound to lipid in discoidal high-density lipoprotein particles. *Biochemistry 41*, 10895−10905.
8. Cheung, M. C., Segrest, J. P., Albers, J. J., Cone, J. T., Brouillette, C. G., Chung, B. H., Kashyap, M., Glasscock, M. A., and Anantharamaiah, G. M. (1987) Characterization of high-density lipoprotein subspecies: structural studies by single vertical spin ultracentrifugation and immunoaffinity chromatography. *J. Lipid Res. 28*, 913−929.
9. Castro, G. R., and Fielding, C. J. (1988) Early incorporation of cell-derived cholesterol into pre-beta-migrating high-density lipoprotein. *Biochemistry 27*, 25−29.
10. Wang, N., Silver, D. L., Thiele, C., and Tall, A. R. (2001) Atp-binding cassette transporter a1 (abca1) functions as a cholesterol efflux regulatory protein. *J. Biol. Chem. 276*, 23742−23747.
11. Jonas, A., Zorich, N. L., Kezdy, K. E., and Trick, W. E. (1987) Reaction of discoidal complexes of apolipoprotein A-I and various phosphatidylcholines with lecithin cholesterol acyltransferase. Interfacial effects. *J. Biol. Chem. 262*, 3969−3974.
12. Brouillette, C. G., Jones, J. L., Ng, T. C., Kercret, H., Chung, B. H., and Segrest, J. P. (1984) Structural studies of apolipoprotein A-I/phosphatidylcholine recombinants by high-field proton NMR,

nondenaturing gradient gel electrophoresis, and electron microscopy. *Biochemistry 23*, 359−367.
13. Jonas, A., Kezdy, K. E., and Wald, J. H. (1989) Defined apolipoprotein A-I conformations in reconstituted high-density lipoprotein discs. *J. Biol. Chem. 264*, 4818−4824.
14. Kunitake, S. T., Chen, G. C., Kung, S. F., Schilling, J. W., Hardman, D. A., and Kane, J. P. (1990) Pre-beta high-density lipoprotein. Unique disposition of apolipoprotein A-I increases susceptibility to proteolysis. *Arteriosclerosis 10*, 25−30.
15. Dalton, M. B., and Swaney, J. B. (1993) Structural and functional domains of apolipoprotein A-I within high-density lipoproteins. *J. Biol. Chem. 268*, 19274−19283.
16. Calabresi, L., Meng, Q. H., Castro, G. R., and Marcel, Y. L. (1993) Apolipoprotein A-I conformation in discoidal particles: evidence for alternate structures. *Biochemistry 32*, 6477−6484.
17. Curtiss, L. K., Bonnet, D. J., and Rye, K. A. (2000) The conformation of apolipoprotein A-I in high-density lipoproteins is influenced by core lipid composition and particle size: a surface plasmon resonance study. *Biochemistry 39*, 5712−5721.
18. Davidson, W. S., Arnvig-McGuire, K., Kennedy, A., Kosman, J., Hazlett, T. L., and Jonas, A. (1999) Structural organization of the N-terminal domain of apolipoprotein A-I: studies of tryptophan mutants. *Biochemistry 38*, 14387−14395.
19. Panagotopulos, S. E., Witting, S. R., Horace, E. M., Nicholas, M. J., and Sean, D. W. (2002) Bacterial expression and characterization of mature apolipoprotein A-I. *Protein Expr. Purif. 25*, 353−361.
20. Maiorano, J. N., and Davidson, W. S. (2000) The orientation of helix 4 in apolipoprotein A-I-containing reconstituted high-density lipoproteins. *J. Biol. Chem. 275*, 17374−17380.
21. Sokoloff, L., and Rothblat, G. H. (1974) Sterol to phospholipid molar ratios of L cells with qualitative and quantitative variations of cellular sterol. *Proc. Soc. Exp. Biol. Med. 146*, 1166−1172.
22. Davidson, W. S., Rodrigueza, W. V., Lund-Katz, S., Johnson, W. J., Rothblat, G. H., and Phillips, M. C. (1995) Effects of acceptor particle size on the efflux of cellular free cholesterol. *J. Biol. Chem. 270*, 17106−17113.
23. Markwell, M. A., Haas, S. M., Bieber, L. L., and Tolbert, N. E. (1978) A modification of the Lowry procedure to simplify protein determination in membrane and lipoprotein samples. *Anal. Biochem. 87*, 206−210.
24. Sparks, D. L., Lund-Katz, S., and Phillips, M. C. (1992) The charge and structural stability of apolipoprotein A-I in discoidal and spherical recombinant high-density lipoprotein particles. *J. Biol. Chem. 267*, 25839−25847.
25. Davidson, W. S., Hazlett, T., Mantulin, W. W., and Jonas, A. (1996) The role of apolipoprotein AI domains in lipid binding. *Proc. Natl. Acad. Sci. U.S.A. 93*, 13605−13610.
26. Lehrer, S. S. (1971) Solute perturbation of protein fluorescence. The quenching of the tryptophyl fluorescence of model compounds and of lysozyme by iodide ion. *Biochemistry 10*, 3254−3263.
27. Panagotopulos, S. E., Horace, E. M., Maiorano, J. N., and Davidson, W. S. (2001) Apoliprotein A-I adopts a belt-like orientation in reconstituted high density lipoproteins. *J. Biol. Chem. 276*, 42965−42970.
28. Matz, C. E., and Jonas, A. (1982) Reaction of human lecithin cholesterol acyltransferase with synthetic micellar complexes of apolipoprotein A-I, phosphatidylcholine, and cholesterol. *J. Biol. Chem. 257*, 4541−4546.
29. Nichols, A. V., Gong, E. L., Blanche, P. J., Forte, T. M., and Shore, V. G. (1984) Interaction of model discoidal complexes of phosphatidylcholine and apolipoprotein A-I with plasma components. Physical and chemical properties of the transformed complexes. *Biochim. Biophys. Acta 793*, 325−337.
30. Gilardi, G., Mei, G., Rosato, N., Canters, G. W., and Finazzi-Agro, A. (1994) Unique environment of Trp48 in *Pseudomonas aeruginosa* azurin as probed by site-directed mutagenesis and dynamic fluorescence spectroscopy. *Biochemistry 33*, 1425−1432.
31. Sorci-Thomas, M. G., Curtiss, L., Parks, J. S., Thomas, M. J., Kearns, M. W., and Landrum, M. (1998) The hydrophobic face orientation of apolipoprotein A-I amphipathic helix domain 143−164 regulates lecithin: cholesterol acyltransferase activation. *J. Biol. Chem. 273*, 11776−11782.
32. Sorci-Thomas, M. G., Curtiss, L., Parks, J. S., Thomas, M. J., and Kearns, M. W. (1997) Alteration in apolipoprotein A-I 22-mer repeat order results in a decrease in lecithin: cholesterol acyltransferase reactivity. *J. Biol. Chem. 272*, 7278−7284.
33. Jonas, A. (1998) Regulation of lecithin cholesterol acyltransferase activity. *Prog. Lipid Res. 37*, 209−234.
34. Corsico, B., Toledo, J. D., and Garda, H. A. (2001) Evidence for a central apolipoprotein A-I domain loosely bound to lipids in discoidal lipoproteins that is capable of penetrating the bilayer of phospholipid vesicles. *J. Biol. Chem. 276*, 16978−16985.
35. Segrest, J. P. (1977) Amphipathic helixes and plasma lipoproteins: thermodynamic and geometric considerations. *Chem. Phys. Lipids 18*, 7−22.
36. Wlodawer, A., Segrest, J. P., Chung, B. H., Chiovetti, R. J., and Weinstein, J. N. (1979) High-density lipoprotein recombinants: evidence for a bicycle tire micelle structure obtained by neutron scattering and electron microscopy. *FEBS Lett. 104*, 231−235.
37. Koppaka, V., Silvestro, L., Engler, J. A., Brouillette, C. G., and Axelsen, P. H. (1999) The structure of human lipoprotein A-I. Evidence for the "belt" model. *J. Biol. Chem. 274*, 14541−14544.
38. Li, H., Lyles, D. S., Thomas, M. J., Pan, W., and Sorci-Thomas, M. G. (2000) Structural determination of lipid-bound ApoA-I using fluorescence resonance energy transfer. *J. Biol. Chem. 275*, 37048−37054.
39. Davidson, W. S., and Hilliard, G. M. (2003) The spatial organization of apolipoprotein A-I on the edge of discoidal high-density lipoprotein particles. *J. Biol. Chem. 278*, 27199−27207.
40. Jonas, A., Wald, J. H., Toohill, K. L., Krul, E. S., and Kezdy, K. E. (1990) Apolipoprotein A-I structure and lipid properties in homogeneous, reconstituted spherical and discoidal high-density lipoproteins. *J. Biol. Chem. 265*, 22123−22129.
41. Li, H. H., Lyles, D. S., Pan, W., Alexander, E., Thomas, M. J., and Sorci-Thomas, M. G. (2002) ApoA-I structure on discs and spheres. Variable helix registry and conformational states. *J. Biol. Chem. 277*, 39093−39101.
42. Klon, A. E., Segrest, J. P., and Harvey, S. C. (2002) Molecular dynamics simulations on discoidal HDL particles suggest a mechanism for rotation in the apo A-I belt model. *J. Mol. Biol. 324*, 703−721.
43. Segrest, J. P., De Loof, H., Dohlman, J. G., Brouillette, C. G., and Anantharamaiah, G. M. (1990) Amphipathic helix motif: classes and properties. *Proteins 8*, 103−117.
44. Roberts, L. M., Ray, M. J., Shih, T. W., Hayden, E., Reader, M. M., and Brouillette, C. G. (1997) Structural analysis of apolipoprotein A-I: limited proteolysis of methionine-reduced and -oxidized lipid-free and lipid-bound human apo A-I. *Biochemistry 36*, 7615−7624.
45. Sparks, D. L., and Phillips, M. C. (1992) Quantitative measurement of lipoprotein surface charge by agarose gel electrophoresis, *J. Lipid Res. 33*, 123−130.

BI0496642